


 Cite this: *RSC Adv.*, 2021, **11**, 19682

# Fungal melanin as a biocompatible broad-spectrum sunscreen with high antioxidant activity†

 Jeong-Joo Oh,<sup>a</sup> Jee Young Kim,<sup>a</sup> Seung Han Son,<sup>b</sup> Won-Jo Jung,<sup>c</sup> Da Hee Kim,<sup>a</sup> Jin-Woo Seo<sup>a</sup> and Gyu-Hyeok Kim<sup>ib</sup>\*<sup>a</sup>

Melanin is considered a bio-inspired dermo-cosmetic component due to its high UV absorption and antioxidant activity. Among various melanin sources, fungal melanin is a promising candidate for sunscreen because of its sustainability and scalability; however, quantitative assessment of its function has not yet been sufficiently explored. In this study, melanin samples derived from *Amorphotheca resinae* were prepared, followed by the evaluation of their sunscreen performance, antioxidant activity, and cytotoxicity. Melanin-blended cream was prepared by blending a melanin suspension and a pure cream. The cream showed an *in vitro* sun protection factor value of 2.5 when the pigment content was 5%. The cream showed a critical wavelength of approximately 388 nm and a UVA/UVB ratio of more than 0.81, satisfying the broad-spectrum sunscreen requirement. Oxygen radical absorbance capacity assays indicated that fungal melanin had antioxidant activity similar to ascorbic acid but higher than reduced glutathione. Fungal melanin had no statistically significant cytotoxicity to human keratinocyte cell lines until 72 h of exposure, even at a concentration of 4 mg mL<sup>-1</sup>. Consequently, melanin pigment can be used as a biocompatible broad-spectrum sunscreen with high antioxidant activity and as a practical alternative in dermo-cosmetic formulations.

 Received 1st April 2021  
 Accepted 23rd May 2021

DOI: 10.1039/d1ra02583j

[rsc.li/rsc-advances](http://rsc.li/rsc-advances)

## 1. Introduction

In line with the growing social awareness of the deleterious effects caused by ultraviolet (UV) radiation on the skin, the usage of sunscreens has grown continuously.<sup>1,2</sup> In the market, there are physical and chemical sunscreens; working mechanisms of active ingredients determine the sunscreen type.<sup>3</sup> The former contains inorganic particles such as zinc oxide, which prevent UV radiation *via* scattering and reflection.<sup>4</sup> The latter includes active ingredients such as avobenzone, homosalate, octisalate, and octocrylene and depends on transforming UV radiation into heat for skin protection.<sup>5</sup> The latter is less prone to leaving unpleasant white residue on the skin and thus considered cosmetically acceptable.<sup>6</sup> Owing to these advantages, chemical sunscreens hold a larger share of the sunscreen market.<sup>6,7</sup>

Despite their advantages, chemical sunscreens have raised some concerns due to the potential adverse effects of their ingredients on human health and ecosystems.<sup>8</sup> The investigation

of the potential cytotoxicity of organic sunscreens has revealed that their post-UV absorption leads to the formation of photo-unstable intermediates such as free radicals, negatively affecting the skin *via* inflammatory reactions.<sup>9–14</sup> Several cases of sunscreen occurrence in aquatic ecosystems have been reported.<sup>15,16</sup> Their accumulating concentrations in the aquatic environment are reported to cause bleaching in coral reefs and endocrine system disorders in organisms.<sup>17–19</sup> After recognizing these adverse environmental effects, some states in the United States passed a law prohibiting the sale of sunscreens that include oxybenzone or octinoxate. Similar measures are now being actively discussed in other countries such as Brazil and the European Union.<sup>8</sup> Therefore, it is not surprising that natural ingredients without such adverse effects have emerged as appealing alternatives to synthetic ingredients.<sup>20–22</sup>

Melanin, which is a naturally occurring pigment, has photoprotective properties of broad-spectrum absorbance and remarkable antioxidant activity.<sup>23,24</sup> Melanogenesis in human skin absorbs 50–75% of UV radiation, and the values of its sun photoprotection factor (SPF) are projected to be 1.5–2.0.<sup>23,25</sup> This pigment in human skin scavenges free radicals generated by UV absorption.<sup>26</sup> Likewise, some microorganisms form intracellular melanin as a putative biological shield to prevent UV damage and to scavenge free radicals.<sup>27</sup> Due to its intrinsic multifunctional behavior, numerous studies have been carried out to utilize melanin in the dermo-cosmetic and biomedical fields.<sup>28</sup>

<sup>a</sup>Division of Environmental Science & Ecological Engineering, College of Life Sciences & Biotechnology, Korea University, 145, Anam-ro, Seongbuk-gu, Seoul 02841, Korea. E-mail: lovewood@korea.ac.kr; Fax: +82 2 3290 9753; Tel: +82 2 3290 3014

<sup>b</sup>Department of Life Science and Research Institute for Natural Sciences, Hanyang University, Seoul 04763, Korea

<sup>c</sup>Department of Advanced Materials Chemistry, Korea University, Sejong 30019, Korea

† Electronic supplementary information (ESI) available. See DOI: 10.1039/d1ra02583j



Fungal melanin, among various sources of melanin, can be a promising candidate for a bio-inspired sunscreen with anti-oxidant activity because it is environmentally sustainable and industrially scalable.<sup>29</sup> Compared to synthetic sunscreens, which entail complex procedures with many ingredients, the preparation of bio-inspired sunscreens is relatively simple and requires natural raw materials. Melanin has no hazardous effects on living organisms in the ecosystem after its disposal which is attributable to its outstanding biocompatibility.<sup>30</sup> Moreover, in terms of its scalable production, there are well-established ways for the production of various fungal melanins. For example, the extraction and purification process from commercial and waste mushrooms yields up to approximately 10% of the dry biomass.<sup>31,32</sup> Also, there has been a well-established method to produce extracellular melanins in cultivation media using promising fungal isolates such as *Amorphotheca resinae* and *Armillaria cepistipes*.<sup>33,34</sup> In spite of the potentiality for fungal melanins as sunscreen agents, the sunscreen performance of fungal melanins has not yet been explored quantitatively.

Herein, we formulated fungal melanin-blended cream and investigated its sunscreen performance for predicting the potential of dermatological uses. The pigment with homogeneous size distribution was initially prepared, and their UV absorbance properties and a plausible adsorption mechanism were characterized *via* microscopy and spectroscopy. The sunscreen performance of melanin-blended cream was then characterized as measurements of *in vitro* SPF, UVA/UVB ratio, and critical wavelength ( $\lambda_c$ ). The UV-shielding properties were assessed under artificial UV light. The antioxidant activity and cytotoxicity of melanin were evaluated for application of dermatological uses. The results of this study will provide necessary information on the UV absorbance of fungal melanin and its potential as dermatological ingredients.

## 2. Materials and methods

### 2.1. Preparation of fungal melanin from *A. resinae*

Melanin derived from *A. resinae* KUC3009 was chosen because it is produced in a large amount and is easy to purify, which is a prerequisite for commercial application.<sup>34</sup> Spores of strain *A. resinae* were isolated by scraping 10 days-old cultures on potato dextrose agar using 0.02% Tween® 80. Thereafter, 1 mL of spore suspension ( $10^6$  spores per mL) was prepared and then inoculated into each flask containing 100 mL culture media (2% glucose, 1% peptone, and 0.5% yeast extract). The inoculated cultures were shaken at 150 rpm on a rotary shaker at 27 °C for 14 d. Cell-free culture media were obtained through centrifugation. The pH of the culture media was acidified to pH 2.0 with 1 M HCl and then incubated for 24 h. After the occurrence of melanin precipitates, they were collected through repetitive centrifugation. The acid-hydrolysing was applied to the obtained melanin by incubating in 6 M HCl at 100 °C for 2 h to exclude unnecessary cellular and proteinaceous components. Melanin precipitates were recollected through centrifugation. These pigments were repeatedly rinsed with deionized distilled water and lyophilized. For the formulation of melanin-blended

cream, melanin suspensions of desired concentrations were prepared as follows. The desired amounts of melanin were suspended in 0.5 M NH<sub>4</sub>OH solutions and then sonicated using an STH-750 s ultrasonic homogenizer (Sonictopia, Cheongju, Korea) at 20 kHz, 480 W for 20 min. The three times of sonication procedure cycles were conducted for a homogenous texture.

### 2.2. Characterization of fungal melanin derived from *A. resinae*

**2.2.1. Morphological characterization.** Morphological characterization of the melanin suspension was performed using a transmission electron microscope (TEM) and a particle-size analyzer with a dynamic light scattering method. Observations of melanin suspension were conducted using JEM 2100F (JEOL, Tokyo, Japan). TEM images of melanin in NH<sub>4</sub>OH solution were recorded after the solution was placed on a carbon-coated copper TEM grid. The particle size range of melanin and its polydispersity were measured using a 90 Plus Particle Size Analyzer (Brookhaven Instruments Corporation, Holtsville, NY, USA).

**2.2.2. Spectroscopic characterization.** The absorption characteristics of melanin suspension were investigated using a UV-vis spectrophotometric approach. The absorbance of melanin in 0.5 M NH<sub>4</sub>OH solution was obtained using the GENESYS™ 10S UV-Vis spectrophotometer (ThermoFisher Scientific, Pittsburgh, PA, USA). The spectra were recorded within the range of 280 to 800 nm at 1 nm intervals. The structural characteristics of melanin were investigated by Fourier transform-infrared spectroscopy (FT-IR). The potassium bromide was shaped as pellets and then brushed with melanin suspensions. The spectra measurement for pellets was carried out using a Nicolet 6700 spectrometer (ThermoFisher Scientific, Pittsburgh, PA, USA).

**2.2.3. Determination of antioxidant activity.** The antioxidant activities of melanin in NH<sub>4</sub>OH solution were investigated using an oxygen radical absorption capacity (ORAC) assay, which is commonly applied to evaluate cosmetic antioxidant capacity.<sup>35</sup> Reduced glutathione (GSH) and L-ascorbic acid, commonly used antioxidant agents in cosmetic formulations, were set as the control group.<sup>36</sup> The ORAC assay was conducted according to previous studies.<sup>37</sup> A solution of 78 nM fluorescein (FL) and 221 mM 2,2'-azobis(2-amidinopropane) dihydrochloride (AAPH) radical was prepared daily. A 20 μM Trolox (6-hydroxy-2,5,7,8-tetramethylchroman-2-carboxylic acid) solution was set as a reference. In each well of a 96-well plate, 50 μL of FL (78 nM), samples with different concentrations (melanin, 0.0125–0.2 mg L<sup>-1</sup>; GSH, 0.025–0.2 mg L<sup>-1</sup>; ascorbic acid, 0.0125–0.1 mg L<sup>-1</sup>), blank (75 mM phosphate buffer) or Trolox standard, were placed and mixed. Then, the incubation was conducted at 37 °C for 20 min. After the addition of 25 μL AAPH in each well, fluorescence intensity was measured immediately. Until the intensity was less than 5% of the initial intensity, the intensity was measured every 5 min interval, on a fluorescence filter with an excitation wavelength of 485 nm and an emission wavelength of 535 nm.



The calculation of the ORAC values expressed as  $\mu\text{M}$  Trolox equivalents ( $\mu\text{M TE g}^{-1}$ ) was carried out using the formula by:  $\text{ORAC } (\mu\text{M TE g}^{-1}) = C_{\text{Trolox}}(\text{AUC}_{\text{sample}} - \text{AUC}_{\text{blank}})k/(\text{AUC}_{\text{Trolox}} - \text{AUC}_{\text{blank}})$ , where  $C_{\text{Trolox}}$  denotes the concentration ( $\mu\text{M}$ ) of Trolox (20  $\mu\text{M}$ ) and  $k$  denotes the sample dilution factor. AUC represents the area below the fluorescence decay curve of the sample, blank, and Trolox, respectively, and it was calculated using the formula by:  $\text{AUC} = (0.5 + f_5/f_0 + f_{10}/f_0 + \dots + f_{n+5}/f_0)5$ , where  $f_0$  and  $f_n$  connote the initial fluorescence and the fluorescence at time  $n$ , respectively.

**2.2.4. Determination of cytotoxicity.** The cytotoxic effect of melanin in  $\text{NH}_4\text{OH}$  solution was evaluated in the HaCaT cell line (San Diego, CA, USA), which is widely being employed in predicting cytotoxicity of ingredients for cosmetic application, *via* the MTT (3-(4,5-dimethylthiazol-2-yl)-2,5-diphenyl tetrazolium bromide) assay with reference to previous studies.<sup>38–40</sup> The HaCaT cells were cultured in Dulbecco's modified Eagle's medium at 37 °C with 5%  $\text{CO}_2$ . 10% fetal bovine serum and 1% penicillin–streptomycin (10 000 U  $\text{mL}^{-1}$ ) were supplemented to the medium prior to cell culture. The cells were then plated separately in flat-bottomed 96-well culture plates at a concentration of  $3 \times 10^3$  cells per well. Different concentrations of melanin suspension (0–4  $\text{mg mL}^{-1}$ ) were treated to the cells after 24 h incubation. After the treatment of 24, 48, 72, and 96 h, the medium was aspirated. The serum-free medium containing MTT (5  $\text{mg mL}^{-1}$ ) was added and incubated in a  $\text{CO}_2$  incubator for 3 h at 37 °C. The medium containing MTT was discarded, and the newly formed crystals were dissolved in 100  $\mu\text{L}$  of dimethyl sulfoxide. The formazan concentration was estimated spectrophotometrically at 490 nm using a VarioSkan Flash Spectral Scanning Multimode Reader (ThermoFisher Scientific, Pittsburgh, PA, USA).

### 2.3. Formulation of melanin-blended cream

Melanin-blended cream was formulated using a method of previous studies.<sup>21</sup> All melanin-blended cream samples were prepared by blending a melanin suspension with pure cream. The entire blending process was performed with continuous stirring under darkroom conditions. The pure cream was purchased from the Korean drug markets. Their ingredients, both active and inactive, are shown in Table S1.†

### 2.4. Determination of *in vitro* SPF, UVA/UVB, and critical wavelength of melanin-blended cream

*In vitro* SPF was determined using the method of Diffey and Robson; 25 mg of prepared melanin-blended cream was transferred to 12.5  $\text{cm}^2$  3M Transpore™ tape stickered on the 2 mm-thickness quartz slides.<sup>41</sup> The prepared cream was then evenly distributed on the surface using a cot-coated finger. The sample was put under darkroom conditions for 20 min. Then, the UV transmittance was measured using a Cary 5000 UV-Vis-NIR spectrophotometer (Agilent Technologies, Santa Clara, CA, USA). Transmittance per 1 nm was collected at wavelengths in the UV range for each scan. The analyses were performed in triplicate, and three spots per slide were measured. The *in vitro* SPF value was determined using the equation by: *in vitro*

$\text{SPF} = \frac{\sum_{290}^{400} E_{\lambda} S_{\lambda}}{\sum_{290}^{400} E_{\lambda} S_{\lambda} T}$ , where  $E_{\lambda}$ ,  $S_{\lambda}$ , and  $T_{\lambda}$  denote the CIE erythral spectral effectiveness, the solar spectral irradiance, and the spectral transmittance of the sample, respectively.

The critical wavelength ( $\lambda_c$ ) refers to the first value at which the ratio  $R \geq 0.9$ , corresponding to 90% or above from the integral curve of absorbance. The potential of UVA protection can be measured and evaluated as a broad spectrum when  $\lambda_c > 370$  nm.  $R$  is defined across the 290–400 nm spectrum using the following equation by:  $R = \frac{\int_{290}^{\lambda_c} A_{\lambda} d\lambda / \int_{290}^{400} A_{\lambda} d\lambda}{\int_{290}^{\lambda_c} A_{\lambda} d\lambda / \int_{290}^{320} A_{\lambda} d\lambda}$ , where  $A_{\lambda}$  is the spectral absorbance value.

The UVA/UVB ratio, the total absorption in the UVA to that in the UVB, represents the UVA protection in addition to the SPF values.<sup>42</sup> Such ratios were obtained using the following equation by:  $\text{UVA/UVB ratio} = \frac{(\int_{320}^{400} A_{\lambda} d\lambda / \int_{320}^{400} d\lambda)}{(\int_{290}^{320} A_{\lambda} d\lambda / \int_{290}^{320} d\lambda)}$ .

### 2.5. Evaluation of UV shielding performance of melanin-blended cream

The UV-shielding performance of the melanin-blended cream was measured based on the degradation behavior of the Rhodamine B solution under UVA and UVB irradiation according to the previous studies with slight modifications.<sup>43,44</sup> Melanin-blended cream (25 mg) was evenly distributed onto a 12.5  $\text{cm}^2$  3M Transpore™ tape attached to quartz slides of 2 mm thickness. After drying under darkroom conditions for 20 min, the slides were placed on top of the  $10^{-5}$  M Rhodamine B solution with 1% hydrogen peroxide. UVA and UVB irradiation were applied with an F4T5 blacklight and a G4T5 E, respectively (Sankyo Denki Co. Ltd., Japan). At a distance of 10 cm, the former source emits in the range of 315–400 nm with an output peak at 360 nm, resulting in an irradiance value of 11  $\text{mW cm}^{-2}$ . At a distance of 10 cm, the latter source emits in the range of 280–360 nm with an output peak at 306 nm, resulting in an irradiance value of 5.5  $\text{mW cm}^{-2}$ . Using the absorbance of the dye solution measured at 554 nm, the UV-shielding performance ( $I$ ) was determined by the following equation:  $I (\%) = 100 \times A_t/A_0$ , where  $A_0$  and  $A_t$  connote the absorbance of the initial solution and that of the solution protected with the slides at time  $n$ , respectively.

## 3. Results and discussion

### 3.1. Formation and characterization of melanin pigment with homogeneous size distribution

We prepared fungal melanin from *A. resiniae* in the powder form after purification (Fig. S1†). However, its form did not ensure a homogeneous size distribution in aqueous solutions, which is a prerequisite for the formulation of melanin-blended sunscreen. Subsequently, ultrasonication treatment of the pigment in the  $\text{NH}_4\text{OH}$  solution was conducted considering that melanin can disperse well only in the alkali solution. After preparation of the melanin suspension, morphological characterization of fungal melanin was conducted to confirm the homogeneous distribution. After ultrasonication for the formulation of homogeneous solutions, the pigment in the solution was dispersed to irregularly shaped particles with



lengths of 50–400 nm, some of which formed aggregates (Fig. 1A). The average size of melanin particles was  $146.8 \pm 2.4$  nm. The distribution of their sizes was relatively even in the range of 50–400 nm (Fig. 1B), which ensures the homogeneity of the melanin pigment in the suspension.

To explore the optical properties of fungal melanin, we also characterized the absorbance characteristics of the pigment derived from *A. resiniae*. The absorbance spectra of melanin suspensions at different concentrations are presented in Fig. 1C. Fungal melanin derived from *A. resiniae* had high optical absorbance in the UV regions, which was proportional to its concentration. The spectra featured a single monotonic absorbance, including a gradual increase from 800 to 600 nm and a noticeable increase from 600 to 285 nm. The spectrum had a maximum peak at approximately 285 nm. These absorbance properties are typically found within the pigment in human skin and synthetic ones assumed to be related to photo-protective functionality.<sup>45</sup>

Scattering would not be responsible for absorption spectra in the UV region because the average size of pigment (approximately 146.5 nm) is not that small enough to be within the Rayleigh scattering.<sup>46</sup> Thus, it is reasonable to assume that high UV absorption of the fungal melanin is attributed to the

chemical structures in molecules rather than scattering, the same as synthetic and human melanin pigments.<sup>47</sup> Our previous study using <sup>13</sup>C nuclear magnetic resonance indicated that indole-based constituents account for the overall structure of pigment, the same as *Sepia* melanin.<sup>34</sup> The detailed structural study was conducted *via* FT-IR to predict which structural components would be responsible for the UV adsorption. The peaks at 3409 and 1540  $\text{cm}^{-1}$  correspond to the amine groups and C–N bonds, which support the structure of the indole-based constituents were shown.<sup>48,49</sup> The bands positioned around  $\sim 3400$   $\text{cm}^{-1}$  indicate the amine groups within the indole-based constituents. The specific species of indole-based constituents were possibly quinones and quinols; the peak observed around 1629  $\text{cm}^{-1}$  is assigned to the carbonyl group (C=O) in the quinone species.<sup>50</sup> The peak at 1228  $\text{cm}^{-1}$  is assigned to the stretching of phenolic alcohols (C–OH).<sup>51</sup> Each peak position at 2921 and 1452  $\text{cm}^{-1}$  is assigned to the multiple alkyl chains, which are additionally bonded to the indole-based species.<sup>52,53</sup> Considering the structural features of the pigment, the high absorption in the UV region is most likely caused by unsaturated carbon bonds present in indole-based constituents.<sup>47</sup> The single broadband absorbance with no distinct chromophoric peaks can be attributed to the structural heterogeneity of

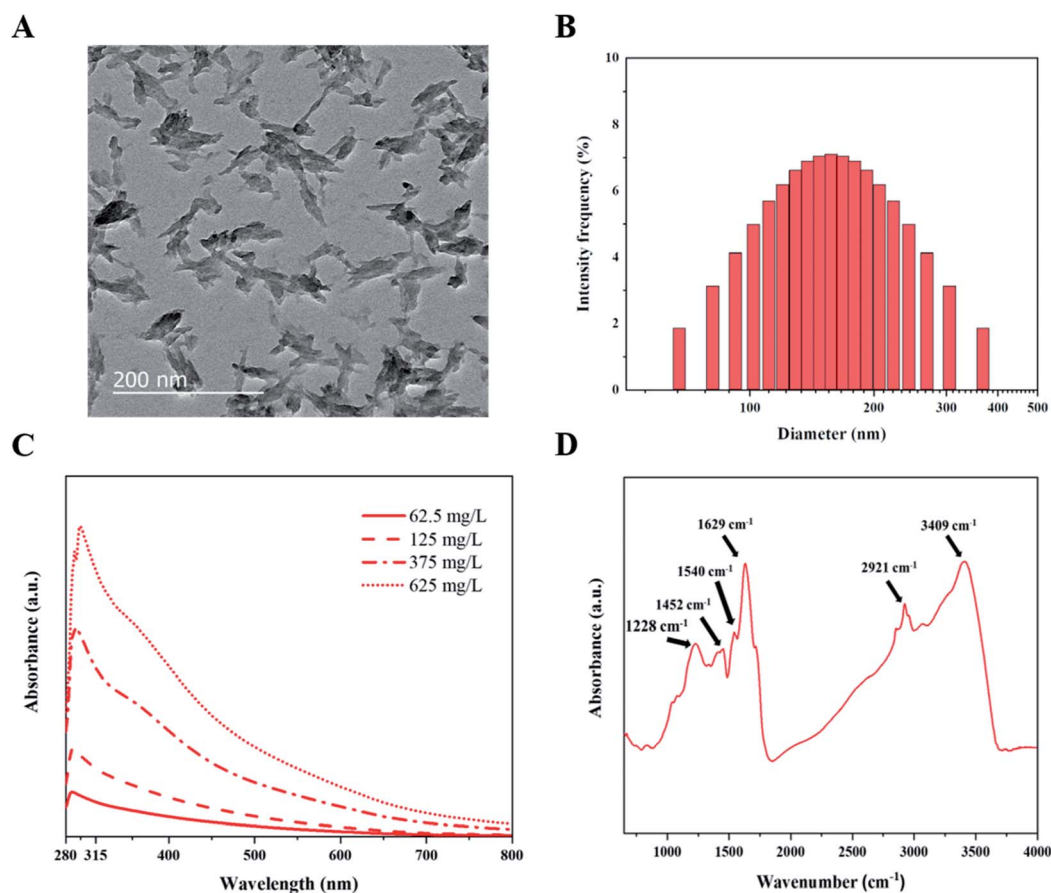


Fig. 1 Formation and characterization of melanin pigment with homogenous size distribution (A) TEM image with  $\times 12\,000$  magnification, (B) size distribution, where y axis is the contribution of scattered light intensity from particles with different sizes to total light intensity, (C) UV-Vis spectrum in the range of 280–800 nm, and (D) FTIR spectrum in the range of 4000–650  $\text{cm}^{-1}$ .



indole-based constituents with a different energy gap between a molecule's highest energy occupied molecular orbital and its lowest energy unoccupied molecular orbital.<sup>54</sup>

### 3.2. Sunscreen performance of fungal melanin-blended cream

Inspired by the high UV absorption of the prepared fungal melanin, we fabricated the melanin-blended cream samples by blending the suspension with pure cream (Fig. 2). Fig. 2 shows the transmittance of the cream blended with different amounts of melanin in the UVA and UVB regions. The pure cream showed a transmittance close to 100% in both UVA and UVB regions. The UV transmittance of the cream decreased in proportion to the melanin content. It was found that the addition of melanin in cream boosted up the SPF values in proportion to the amounts of pigment. The SPF values of pure cream were found approximately 1.0. The melanin-blended cream increased to 2.5 as the melanin content increased to 5% (Table 1). These results indicated that fungal melanin can act as a sunscreen agent.

The melanin-blended creams showed slightly slanted broadband curves, reflecting the absorbance properties of fungal melanin, which have seemingly similar transmittance curves with broad-spectrum sunscreens. The cream samples were quantitatively evaluated as broad-spectrum sunscreen with high UVA effectiveness from the perspective of both critical wavelength and UVA/UVB ratios. In Table 1, their critical wavelength value was higher than 370 nm, which ensured optimal UVA protection. Their UVA/UVB ratio was higher than 0.8, ensuring "maximum" UVA protection for reference to the Boots Star Rating System.<sup>55</sup> These results indicate that fungal melanin is a promising candidate for broad-spectrum sunscreens.

We also confirmed the UV shielding performance of the melanin-blended creams. Fig. 3 shows the photodegradation curves of the Rhodamine B solution protected with the pure cream and melanin-blended creams under UVA and UVB.

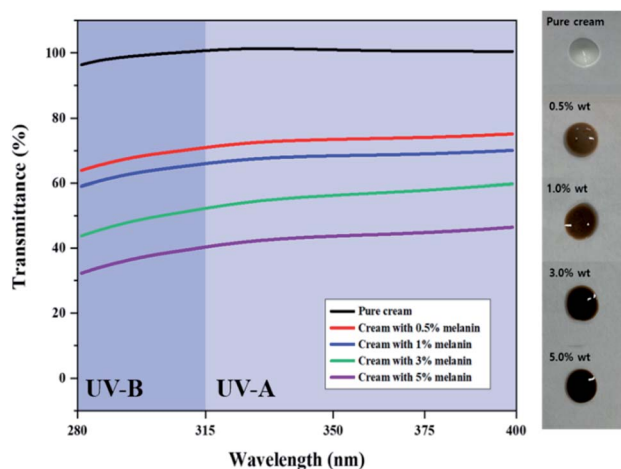


Fig. 2 UV transmittance of the creams blended with different amounts of fungal melanin.

Table 1 *In vitro* SPF values, critical wavelength ( $\lambda_c$ ), and UVA/UVB ratio of cream blended with different amounts of fungal melanin derived from *A. resiniae*

Melanin content (%)	<i>In vitro</i> SPF	Critical wavelength	UVA/UVB ratio
0%	1.0 ± 0.1	—	—
0.5%	1.4 ± 0.1	388.8 ± 0.5	0.88 ± 0.04
1%	1.5 ± 0.1	388.8 ± 0.4	0.90 ± 0.02
3%	2.0 ± 0.2	388	0.84 ± 0.01
5%	2.5 ± 0.1	388	0.87 ± 0.01

Overall, melanin-blended creams prevented the photodegradation of Rhodamine B. The dye solution protected with pure cream underwent considerable photodegradation (near 100%) for 240 and 120 min after UVA and UVB irradiation, respectively. The photodegradation percentage decreased in proportion to the melanin content of the cream. When the cream with 5% melanin protected the dye solution, almost 30% and 20% of the dye remained in the solutions after irradiation. These observations support the important role that fungal melanin absorbs UV irradiation.

However, color and *in vitro* SPF values of melanin-blended cream possibly limited their application. Due to its inherent dark color, the melanin-blended cream would match only with dark skin tone. The dark color of natural melanin was attributed to the high degree of conjugation, causing strong absorption in frequencies of visible lights.<sup>56,57</sup> Especially, lower energy transitions for low frequencies of light are possible through abundant carbonyl bonds (C=O) in quinone moieties.<sup>47,56</sup> It would be homologous to the fungal melanin derived *A. resiniae* considering its quinone moieties identified with an FT-IR study. Besides, the maximum SPF values (2.5) obtained in this study are not sufficient to meet at least 15 requirements when melanin is used as a single active ingredient. The values for fungal melanin were slightly lower than those obtained for the same concentrations of synthetic broad-spectrum sunscreen agents (Table S2†). These results suggest that melanin needs further modifications or mixing with traditional synthetic sunscreen agents to increase the SPF value. Natural sunscreens are often blended with synthetic ones in commercial sunscreen products, diminishing the adverse effects of using synthetic products.<sup>58</sup> Nonetheless, further studies overcoming those concerns should be conducted for the broad application of fungal melanin as dermo-cosmetic components.

### 3.3. Antioxidant activities of fungal melanin

Free radicals in cells can damage molecular components such as proteins and DNA through oxidative chain reactions, which is the main cause of diseases and aging.<sup>59</sup> Because human skin is constantly exposed to external factors such as UV, metal ions, and pathogenic bacteria, which are responsible for the formation of free radicals, using an effective antioxidant in dermo-cosmetic formulations is important.<sup>60</sup> A lot of fungal secondary metabolites are reported to play an important role in



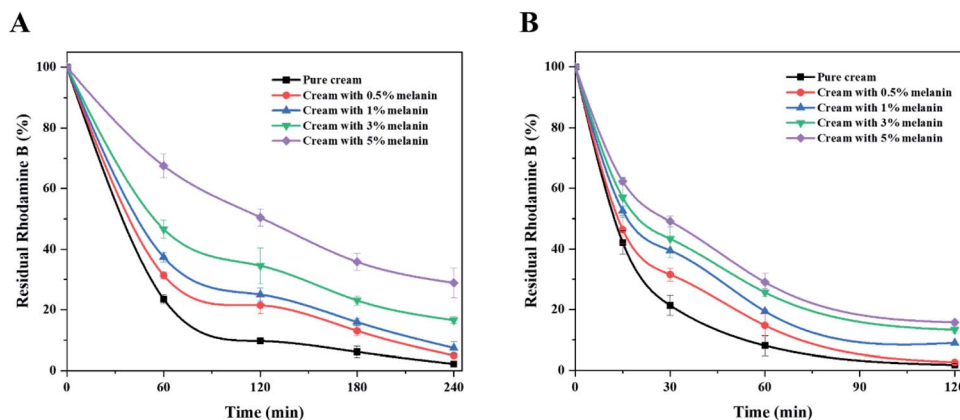


Fig. 3 UV shielding performances of creams blended with different amounts of fungal melanin under (A) UVA light and (B) UVB light.

scavenging free radicals. Thus, we confirmed whether fungal melanin also can act as an antioxidant agent as well as a broad-spectrum sunscreen.

The ORAC assay was selected to measure the antioxidant activity of fungal melanin because this method has advantages in comparison with other methods; this assay utilizes peroxy radicals that are biologically relevant and both the degree and time of the antioxidation reaction are embedded on this assay. Fig. 4 shows the ORAC values of fungal melanin and the conventional antioxidants used in cosmetics. The ORAC value obtained for conventional antioxidants was similar to those in previous studies; the ORAC value of ascorbic acid is approximately two times larger than that of GSH, which validates the results of the assay performed in this study.<sup>60,61</sup> The ORAC value of melanin was  $1105 \mu\text{M TE g}^{-1}$ , slightly larger than that of both ascorbic acid and GSH. There was a statistically significant difference in the ORAC values between melanin and GSH. These results indicated that fungal melanin has potent antioxidant activity, which function lacks in synthetic sunscreens. The antioxidant properties of fungal melanin against peroxy radicals would be attributed to the radical

addition reaction. It was reported that dopa-melanin and cysteinyl-dopa-melanin interacted with most oxidizing radicals with simple one-electron transfer processes possibly due to the presence of unpaired electrons in their chemical structures.<sup>62,63</sup> However, in the case of oxidizing peroxy radicals, melanins interacted *via* radical addition rather than electron transfer. The antioxidant properties would be similar between fungal melanin and dopa-melanin considering the similarity of their chemical structures.

### 3.4. Cell cytotoxicity of fungal melanin

Potential applications of fungal melanin as cosmetic ingredients require them to be harmless. Cell cytotoxicity evaluation of active ingredients should be performed to predict possible skin irritation. There are only a few studies on the cytotoxic effects of fungal melanin on human keratinocytes. In this study, cytotoxic effects of fungal melanin derived from *A. resiniae* were investigated in human keratinocyte HaCaT cells using MTT assays, one of the most common methods to predict the toxicity of a wide range of substances.

Fig. 5 presents the viability of HaCaT cells as a function of the amount of fungal melanin derived from *A. resiniae*. Fungal melanin had no cytotoxic effects on keratinocytes after treatment for 24, 48, and 72 h. There were no significant differences in relative cell viability between the untreated and treated groups after treatment for 24, 48, and 72 h. However, cytotoxic effects of fungal melanin appeared after 96 h of treatment when melanin concentrations were over  $0.4 \text{ mg mL}^{-1}$ . Melanin concentrations over  $0.4 \text{ mg mL}^{-1}$  reduced the relative cell viability of keratinocytes compared to the untreated group. When  $0.4 \text{ mg mL}^{-1}$  of melanin solution was added to HaCaT cells, the melanin dose used in this assay was  $6.67 \text{ ng per cell}$ . These values are significantly larger than the maximum FDA-approved dose of conventional chemical sunscreen agents ( $0.01\text{--}0.1 \text{ ng per cell}$ ), ensuring fungal melanin is much safer than some chemical sunscreens.<sup>40</sup> Besides, the melanin dose per cell was calculated when 5% melanin-blended cream was applied. The assumption for calculation follows as: (1) the amounts of melanin-blended cream per surface follows the

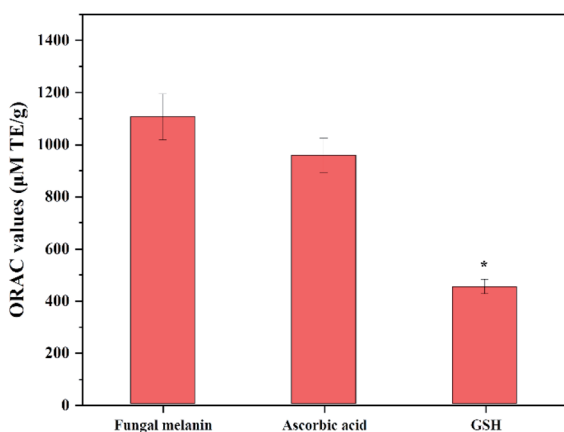


Fig. 4 Antioxidant capacity of fungal melanin derived from *A. resiniae*, ascorbic acid, and GSH. \* indicates significant differences ( $p < 0.05$ ) with respect to fungal melanin.



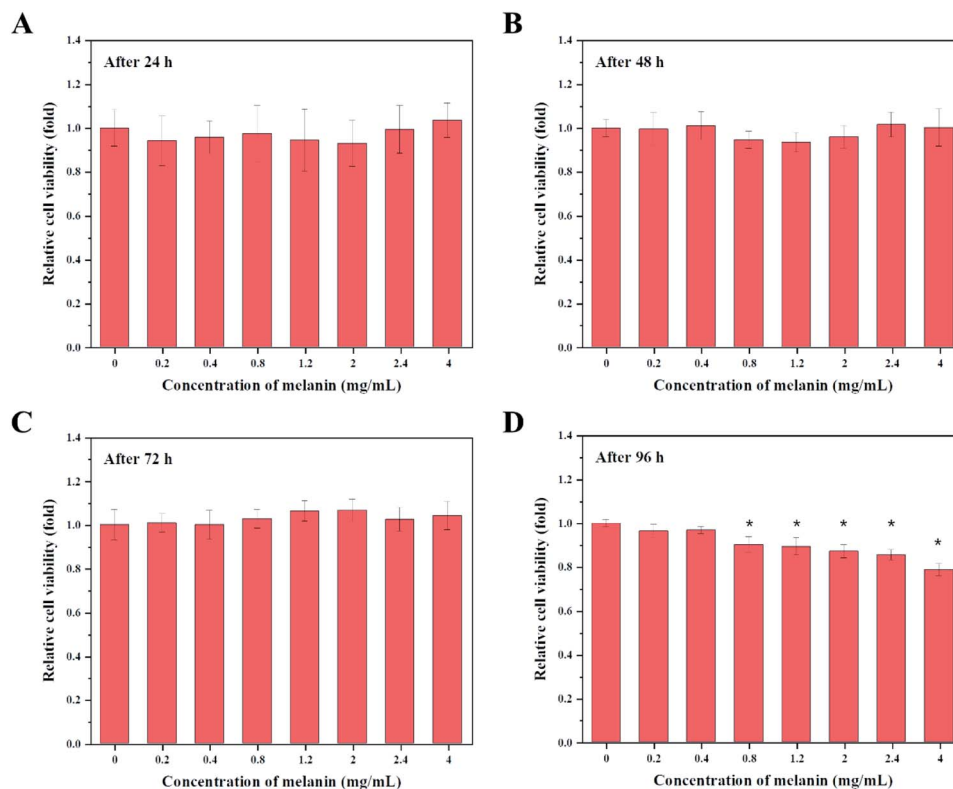


Fig. 5 Cytotoxicity of fungal melanin derived from *A. resiniae* in HaCaT human keratinocytes with an exposure time of (A) 24 h (B) 48 h (C) 72 h, and (D) 96 h. Data shown are mean  $\pm$  standard deviation of five independent experiments. \* indicates statistically significant differences ( $p < 0.05$ ) in comparison with the group incubated with 0 mg mL<sup>-1</sup> of melanin.

method of Diffey and Robson; (2) the epidermal cell density follows the reported empirical number.<sup>64</sup> As a result, the calculated melanin dose was 0.017 ng per cell, which is significantly lower than 6.67 ng per cell, ensuring the safety of 5% of melanin-blended cream. Therefore, the applied melanin-blended cream on the skin can be regarded as a biocompatible cosmetic ingredient.

## 4. Conclusions

Fungal melanin derived from *A. resiniae* was prepared as particles with homogeneous size distribution solutions to serve as sunscreen agents. The melanin-blended cream showed maximum SPF values of 2.5, with a critical wavelength of approximately 388 nm and a UVA/UVB ratio of more than 0.81, satisfying a broad-spectrum sunscreen requirement. Simultaneously, the melanin had higher antioxidant activity than those of conventional antioxidants. The pigment would cause no cytotoxicity towards keratinocytes even at 4 mg mL<sup>-1</sup> after exposure up to 72 h. Consequently, fungal melanin can be utilized as a multi-purpose broad-spectrum sunscreen agent with no cytotoxicity, contributing to replacing or diminishing some synthetic broad-spectrum sunscreens in cosmetic formulations.

## Conflicts of interest

There are no conflicts to declare.

## Acknowledgements

This study was supported by a Korea University Research Grant.

## References

- P. Césarini, *Recent Results Cancer Res.*, 2002, **160**, 70–72.
- U. Osterwalder, M. Sohn and B. Herzog, *Photodermatol., Photoimmunol. Photomed.*, 2014, **30**, 62–80.
- F. P. Gasparro, M. Mitchnick and J. F. Nash, *Photochem. Photobiol.*, 1998, **68**, 243–256.
- G. P. Dransfield, *Inorganic sunscreens, Radiat. Prot. Dosim.*, 2000, **91**, 271–273.
- D. R. Kimbrough, *J. Chem. Educ.*, 1997, **74**, 51–53.
- A. S. Adamson and K. Shinkai, *JAMA*, 2020, **323**, 223–224.
- M. S. Reisch, *Chem. Eng. News*, 2001, **79**, 25–29.
- S. Narla and H. W. Lim, *Photochem. Photobiol. Sci.*, 2020, **19**, 66–70.
- V. F. Sherwood, S. Kennedy, H. Zhang, G. H. Purser and R. J. Sheaff, *Cutaneous Ocul. Toxicol.*, 2012, **31**, 273–279.
- A. Balázs, C. Krifaton, I. Orosz, S. Szoboszlai, R. Kovács, Z. Csenki, B. Urbányi and B. Kriszt, *Ecotoxicol. Environ. Saf.*, 2016, **131**, 45–53.
- K. M. Hanson, E. Gratton and C. J. Bardeen, *Free Radical Biol. Med.*, 2006, **41**, 1205–1212.
- I. Karlsson, L. Hillerström, A. L. Stenfeldt, J. Mårtensson and A. Börje, *Chem. Res. Toxicol.*, 2009, **22**, 1881–1892.



- 13 E. Damiani, L. Rosati, R. Castagna, P. Carloni and L. Greci, *J. Photochem. Photobiol., B*, 2006, **82**, 204–213.
- 14 F. M. Vilela, F. M. Oliveira, F. T. Vicentini, R. Casagrande, W. A. Verri Jr, T. M. Cunha and M. J. Fonseca, *J. Photochem. Photobiol., B*, 2016, **163**, 413–420.
- 15 M. E. Balmer, H.-R. Buser, M. D. Muller and T. Poiger, *Environ. Sci. Technol.*, 2004, **39**, 953–962.
- 16 J. M. Brausch and G. M. Rand, *Chemosphere*, 2011, **82**, 1518–1532.
- 17 N. Bluthgen, N. Meili, G. Chew, A. Odermatt and K. Fent, *Sci. Total Environ.*, 2014, **476**, 207–217.
- 18 M. Coronado, H. De Haro, X. Deng, M. A. Rempel, R. Lavado and D. Schlenk, *Aquat. Toxicol.*, 2008, **90**, 182–187.
- 19 R. Danovaro, L. Bongiorno, C. Corinaldesi, D. Giovannelli, E. Damiani, P. Astolfi, L. Greci and A. Pusceddu, *Environ. Health Perspect.*, 2008, **116**, 441–447.
- 20 M. D. Mota, A. N. da Boa Morte, L. C. R. C. e Silva and F. A. Chinalia, *J. Photochem. Photobiol., B*, 2020, **205**, 111837.
- 21 Y. Qian, X. Qiu and S. Zhu, *Green Chem.*, 2015, **17**, 320–324.
- 22 N. Poulouse, A. Sajayan, A. Ravindran, T. V. Sreechithra, V. Vardhan, J. Selvin and G. S. Kiran, *J. Photochem. Photobiol., B*, 2020, **205**, 111816.
- 23 M. Brenner and V. J. Hearing, *Photochem. Photobiol.*, 2008, **84**, 539–549.
- 24 J. Bustamante, L. Bredeston, G. Malanga and J. Mordoh, *Pigm. Cell Res.*, 1993, **6**, 348–353.
- 25 K. H. Kaidbey, P. P. Agin, R. M. Sayre and A. M. Kligman, *J. Am. Acad. Dermatol.*, 1979, **1**, 249–260.
- 26 T. Herrling, K. Jung and J. Fuchs, *Spectrochim. Acta, Part A*, 2008, **69**, 1429–1435.
- 27 Q. Gao and F. Garcia-Pichel, *Nat. Rev. Microbiol.*, 2011, **9**, 791–802.
- 28 C. Cavallini, G. Vitiello, B. Adinolfi, B. Silvestri, P. Armanetti, P. Manini, A. Pezella, M. d'Ischia, G. Luciani and L. Menichetti, *Nanomaterials*, 2020, **10**, 1518.
- 29 R. J. Cordero and A. Casadevall, *Fungal Biol. Rev.*, 2017, **31**, 99–112.
- 30 F. Solano, *Int. J. Mol. Sci.*, 2017, **18**, 1561.
- 31 R. Prados-Rosales, S. Toriola, A. Nakouzi, S. Chatterjee, R. Stark, G. Gerfen, P. Tumpowsky, E. Dadachova and A. Casadevall, *J. Agric. Food Chem.*, 2015, **63**, 7326–7332.
- 32 X. Liu, R. Hou, D. Wang, M. Mai, X. Wu, M. Zheng and J. Fu, *Nutr. Food Sci.*, 2019, **7**, 3774–3783.
- 33 J. Ribera, G. Panzarasa, A. Stobbe, A. Osypova, P. Rupper, D. Klose and F. W. Schwarze, *J. Agric. Food Chem.*, 2018, **67**, 132–139.
- 34 J. J. Oh, J. Y. Kim, S. L. Kwon, D. H. Hwang, Y. E. Choi and G. H. Kim, *J. Microbiol.*, 2020, **58**, 648–656.
- 35 A. Ratz-Lyko, J. Arct and K. Pytkowska, *Skin Res. Technol.*, 2012, **18**, 421–430.
- 36 N. Nenadis, O. Lazaridou and M. Z. Tsimidou, *J. Agric. Food Chem.*, 2007, **55**, 5452–5460.
- 37 A. Zulueta, M. J. Esteve and A. Frigola, *Food Chem.*, 2009, **114**, 310–316.
- 38 V. Ugartondo, M. Mitjans and M. P. Vinardell, *Bioresour. Technol.*, 2008, **99**, 6683–6687.
- 39 T. Rajkumar, A. Sapi, G. Das, T. Debnath, A. Ansari and J. K. Patra, *J. Photochem. Photobiol., B*, 2019, **193**, 1–7.
- 40 M. Yamada, Y. Mohammed and T. W. Prow, *Adv. Drug Delivery Rev.*, 2020, **153**, 72–86.
- 41 B. L. Diffey and J. Robson, *J. Soc. Cosmet. Chem.*, 1989, **40**, 127–133.
- 42 D. Moyal, *Photochem. Photobiol. Sci.*, 2010, **9**, 516–523.
- 43 Y. Wang, T. Li, P. Ma, H. Bai, Y. Xie, M. Chen and W. Dong, *Chem. Eng.*, 2016, **4**, 2252–2258.
- 44 P. Li, S. Wang and S. Zhou, *J. Mater. Chem. C*, 2020, **8**, 17383–17394.
- 45 J. P. Ortonne, *Br. J. Dermatol.*, 2002, **146**, 7–10.
- 46 J. G. Riesz, J. Gilmore and P. Meredith, *Biophys. J.*, 2006, **90**, 4137–4144.
- 47 P. A. Riley, *Int. J. Biochem. Cell Biol.*, 1997, **29**, 1235–1239.
- 48 S. A. Centeno and J. Shamir, *J. Mol. Struct.*, 2008, **873**, 149–159.
- 49 M. Al Khatib, M. Harir, J. Costa, M. C. Baratto, I. Schiavo, L. Trabalzini, S. Pollini, G. M. Rossolini, R. Basosi and R. Pogni, *Molecules*, 2018, **23**, 1916.
- 50 H. Luo, C. Gu, W. Zheng, F. Dai, X. Wang and Z. Zheng, *RSC Adv.*, 2015, **5**, 13470–13477.
- 51 C. Berthelot, A. Zegeye, D. A. Gaber, M. Chalot, P. Franken, G. M. Kovács, C. Leyval and D. Blaudez, *Microorganisms*, 2020, **8**, 537.
- 52 I. E. Pralea, R. C. Moldovan, A. M. Petrache, M. Ilie, S. C. Heghe, I. Ielciu, R. Nicoară, M. Moldovan, M. Ene, M. Radu, A. Uifălean and C. A. Luga, *Int. J. Mol. Sci.*, 2019, **20**, 3943.
- 53 N. Senesi, T. M. Miano and J. P. Martin, *Biol. Fertil. Soils*, 1987, **5**, 120–125.
- 54 M. L. Tran, B. J. Powell and P. Meredith, *Biophys. J.*, 2006, **90**, 743–752.
- 55 Boots, UK limited, *Measurement Of UVA: UVB Ratios According To The Boots Star Rating System*, Nottingham, UK, 2008.
- 56 E. J. Land, C. A. Ramsden and P. A. Riley, *Methods Enzymol.*, 2004, **378**, 88–109.
- 57 R. J. Cordero and A. Casadevall, *Curr. Biol.*, 2020, **30**, R142–R143.
- 58 A. L. Morocho-Jácome, T. B. Freire, A. C. de Oliveira, T. S. de Almeida, C. Rosado, M. V. R. Velasco and A. R. Baby, *J. Cosmet. Dermatol.*, 2020, 1–9.
- 59 B. N. Amens, *Science*, 1983, **221**, 1256–1264.
- 60 A. V. Benedetto, *Clin. Dermatol.*, 1998, **16**, 129–139.
- 61 C. Pieri, M. Marra, F. Moroni, R. Recchioni and F. Marcheselli, *Life Sci.*, 1994, **55**, 271–276.
- 62 M. Rozanowska, T. Sarna, E. J. Land and T. G. Truscott, *Free Rad. Biol. Med.*, 1999, **26**, 518–525.
- 63 N. E. A. El-Naggar and S. M. El-Ewasy, *Sci. Rep.*, 2017, **7**, 1–19.
- 64 S. B. Hoath and D. G. Leahy, *J. Investig. Dermatol.*, 2003, **121**, 1440–1446.

